Increased GADD153 gene expression during iron chelation-induced apoptosis in Jurkat T- lymphocytes

By: Yuan-Ji Pan, Robin G. Hopkins, George Loo

Pan, Y.-J., Hopkins, R.G. and Loo, G. (2004) Increased GADD153 Gene Expression During Iron Chelation-Induced Apoptosis in Jurkat T-Lymphocytes. *Biochim. Biophys. Acta* 1691, 41-50.

Abstract:

Depriving cells of iron likely stresses them and can result in cell death. To examine the potential relationship between this form of stress and cell death, Jurkat T-lymphocytes were made iron-deficient by exposing them to the iron chelator, deferoxamine (DFO). Such treatment produced evidence of apoptosis, including cell shrinkage, membrane blebbing, chromatin condensation and fragmentation, and also formation of apoptotic bodies. Additionally, proteolytic cleavage of poly(ADP-ribose)polymerase was detected, suggesting involvement of caspases in initiating apoptosis. Indeed, a selective caspase-3 inhibitor prevented the effects of DFO. During the early induction period of apoptosis, GRP78 and HSP70 mRNA expression was not affected. In contrast, there was mainly increased mRNA expression of Growth Arrest and DNA Damage-inducible gene 153 (GADD153), which seemed to be at the level of transcription rather than mRNA stability. Furthermore, fortifying cells with antioxidants did not prevent the increased GADD 153 mRNA expression, and no evidence of single-strand breaks in DNA was found, suggesting that neither reactive oxygen species nor DNA damage was involved in triggering GADD153 gene activation. DFO also caused GADD153 protein to be expressed. Because GADD153 is recognized as a pro-apoptotic gene, these findings generate the notion that GADD153 might help mediate apoptosis in iron-deficient cells.

Keywords: Apoptosis; Caspase-3; GADD153; Iron; Iron deficiency

Article:

1. Introduction

Proper levels of iron are needed by cells to help ensure their viability and proliferative capacity. Iron was initially recognized as an essential trace element for all dividing cells upon finding that DNA synthesis was impaired in human lymphocytes rendered iron-deficient with the iron chelator, deferoxamine (DFO) [1]. This effect of cellular iron deficiency can be attributed to decreased activity of ribonucleotide reductase [2], an iron-dependent enzyme that converts ribonucleotides into deoxyribonucleotides as a prerequisite step for DNA synthesis. As a result, there is growth arrest of iron-deficient cells in the S-phase of the cell cycle [3]. Transcriptional activation of certain genes initiates downstream events leading to the cell cycle arrest. For example, it is known that DFO-induced cellular iron deficiency increases the levels of transcription factor p53, which in turn is directly responsible for activating the CIP-1/WAF-1/SDI1/p21 gene [4]. Subsequently, the p21 gene product inhibits cyclin-dependent kinases that otherwise would promote cell cycle progression.

When impairment of DNA synthesis and cell division becomes critical, iron-deficient cells start to die with evidence of apoptosis being apparent [5,6], but the precise cell death pathway leading to apoptosis has not been completely elucidated. However, there is the suggestion from widely accepted models of apoptosis [7] that iron deficiency-induced apoptosis is initiated by caspases. Activation of caspases is pivotal for later occurrence of the DNA fragmentation and morphological changes characteristic of apoptosis [8]. Hence, because DNA fragmentation [5,6] and morphological changes [6] occur in iron-deficient cells, the possible involvement of caspases, specifically caspase-3, in initiating apoptosis in iron-deficient Jurkat T-lymphocytes was initially investigated to help clarify the chain of events leading to cell death.

It is generally believed that changes in gene expression are important in promoting cell death by apoptosis in iron-deficient cells. In support of this concept, it has been shown that DFO-induced iron deficiency in human breast cancer cells caused apoptosis, which was accompanied by changes in the expression of the pro-apoptotic Bax gene and the anti-apoptotic Bcl-2 gene [9]. However, it is conceivable that other genes could also be involved in mediating apoptosis in iron-deficient cells. Because depriving cells of iron likely creates a stressful cellular environment, another aim of this present study was to determine if the expression of certain stress-response genes is increased in iron-deficient Jurkat T-lymphocytes, in establishing a possible association between the stress-response gene expression and occurrence of cell death.

2. Materials and methods

2.1. Materials

Jurkat T-lymphocytes, a human lymphoblastoid T-cell line, were purchased from ATCC (Rockville, MD). Deferoxamine mesylate (DFO), 2,2-dipyridyl (DPD), and diethylenetriaminepentaacetic acid (DTPA) and all other common reagents were purchased from Sigma Chemical Co. (St. Louis, MO).

2.2. Cell culture and treatment of cells

Jurkat T-lymphocytes were propagated in RPMI-1640 media (Sigma) supplemented with 100 ml/l fetal bovine serum (BioWhittaker Inc., Walkersville, MD), 2 mmol/ l glutamine, 0.54 µmol/l fungizone, 100,000 units/l penicillin, and 100 mg/l streptomycin (last four items from Atlanta Biologicals, Atlanta, GA). To make the cells iron-deficient [10], they were incubated with 100 µM DFO for periods up to 24 h to chelate intracellular iron. DPD and DTPA were utilized similarly to confirm the effects of DFO. Other cell samples were pretreated for 3 h with 600 µM Ac-DEVDCHO (Calbiochem, San Diego, CA) before exposing them to DFO. In some experiments, control cells and cells exposed to DFO were subsequently incubated with actinomycin D (1–5 µg/ml). In other experiments, cells were pretreated with either α-tocopherol (100 µM) for 24 h, or N-acetylcysteine (20 mM) for 2 h, before exposing the cells to DFO.

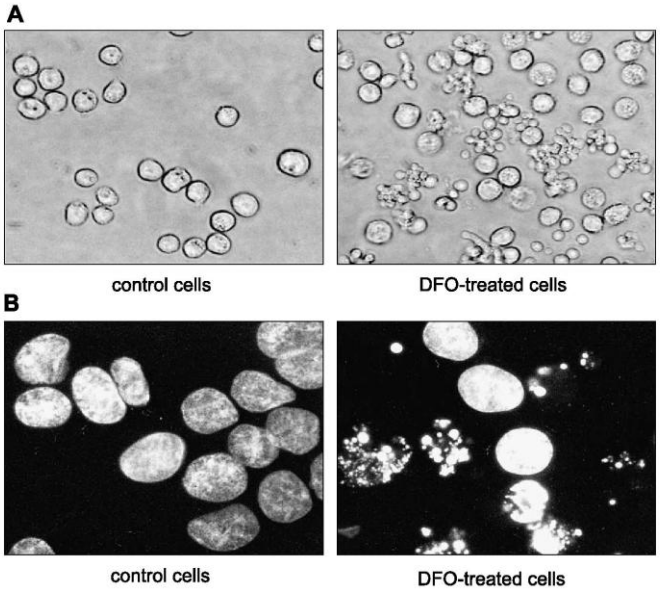

Fig. 1. Morphological appearance of Jurkat T-lymphocytes exposed to DFO. Cells (5×10^5) were incubated either without (control cells) or with 100 µM DFO for 14 h (DFO-treated cells) and then examined by phase-contrast light microscopy (A). To assess chromatin condensation and fragmentation in the cells, the control cells and DFO-treated cells were stained with DAPI and then examined by fluorescence microscopy (B). The results are representative of three different experiments.

2.3. Examination of cells for morphological evidence of apoptosis

Using an Olympus IX-70 inverted microscope/SPOT digital camera system, 200 randomly selected cells were scored visually for the presence of cell shrinkage, plasma membrane blebbing, and/or breakup of the cells into apoptotic bodies, which all are basic markers of apoptosis [11]. Additionally, cells were fixed with 4% formaldehyde and stained with 1 µg/ml 4' ,6-diamidino-2-phenylindole (DAPI) to visualize the extent of chromatin condensation and fragmentation using an Olympus BX-60 fluorescence microscope equipped with a UV filter.

2.4. Detection of proteolytic cleavage of poly-(ADP-ribose)- polymerase (PARP)

At different time points, cells were harvested and washed with ice-cold phosphate-buffered saline (PBS) and then resuspended in PBS containing phenylmethylsulfonyl fluoride (0.1 mg/ml) for sonication on ice. Protein concentration of the lysates was determined with a Bio-Rad DC protein assay kit (Bio-Rad, Hercules, CA). Next, 30 µg of cellular protein was processed for SDS/PAGE using 12% Trisglycine pre-cast gels (Novex, San Diego, CA). The separated proteins on the gels were blotted to nitrocellulose membrane, which was probed with a murine anti-PARP antibody (Santa Cruz Biotechnology, Inc., Santa Cruz, CA) and then with a horseradish peroxidase-conjugated rabbit anti-mouse antibody. Detection of immunosignal was achieved by enhanced chemiluminescence (ECL, Amer-sham, Arlington, IL) using Fuji X-ray film.

2.5. Determination of GRP78, HSP70, and Growth Arrest and DNA Damage-inducible gene 153 (GADD153) mRNA expression

Total RNA was isolated from the cells using a Qiagen RNeasy Mini kit. The expression levels of GRP78, HSP70, and GADD153 mRNA were determined by multiplex relative RT-PCR analysis of total RNA using a Qiagen OneStep RT-PCR kit and gene-specific primers. The PCR primer base sequences for GRP78 and HSP70 were from the NCBI UniSTS data-base of NIH. For GRP78 (UniSTS:48897)— forward primer: GCCTAAGCGGCTGTTTACTG, reverse primer: AACTTCCTACACCAGATGCACA, PCR product size: 174–175 (bp). For HSP70 (UniSTS:70149)—forward primer: TGACTGTCAGGGCTATGCTAT, reverse primer: CAATGTTAAAGTGCCACACAAG, PCR product size: 203 (bp). The GADD153 PCR primer sequences (sense: 5' -GCACCTCCCAGAGCCCTCACTCTCC-3' and anti-sense: 5' -GTCTACTCCAAGCCTTCCCCCTGCG-3') were exactly the same as that used originally by Mertani et al. [12] and gave a PCR product size of 422 bp. Either the β-actin or 18S rRNA QuantumRNA primer/competimer sets (Ambion, Inc., Austin, TX) were used to generate internal standards with cDNA product sizes of 294 and 495 bp, respectively. The RT-PCR conditions for GRP78 and HSP70 were 30 min at 48 °C followed by 15 min at 95 °C (RT), then 0.5 min at 94 °C, 0.5 min at 48 °C, and 1 min at 72 °C for 32 cycles (GRP-78) or 34 cycles (HSP-70) (PCR). The RT-PCR conditions for GADD153 were 30 min at 50 °C followed by 15 min at 95 °C (RT), then 0.5 min at 95 °C, 0.5 min at 60 °C, and 1 min at 72 °C for 25 cycles (PCR). The resulting cDNA products were separated by 2% agarose gel electrophoresis with ethidium bromide staining.

2.6. Determination of GADD153 protein expression

Cells were harvested and washed by centrifugation (500 × g for 5 min) in Hanks Balanced Salt Solution (HBSS). The cell pellets were frozen at — 80C. To prepare whole cell lysates, the frozen cell pellets were thoroughly resuspended in lysis buffer (50 mM Tris–HCl, 150 mM NaCl, 1% Nonidet P-40, 0.25% sodium deoxycholate, 1 mM sodium orthovanadate, 1 mM sodium fluoride, Complete Protease Inhibitor Cocktail from Roche-Boehringer Mannheim, pH 7.4) and left on ice for 30 min. Next, the samples were centrifuged at 16,000 × g for 20 min at 4C. The protein concentrations of the whole cell lysates (supernatant) were determined with a BCA protein assay kit (Pierce Inc.).

For electrophoresis, whole cell lysates (50-µg protein) were loaded into the wells of Novex pre-cast NuPAGE mini-gels (4–12% Bis-Tris). The gel-separated proteins were transferred to nitrocellulose membrane (Pierce), which was then incubated for 1 h at 25 C in blocking buffer consisting of 5% skim milk powder in TBST (20 mM Tris– HCl, 150 mM sodium chloride, 0.05% Tween 20, pH 7.4). Next, the nitrocellulose membrane was incubated overnight at 4C with GADD153 rabbit polyclonal R-20 antibody (Santa Cruz) in blocking buffer (1:5000). After washing in TBST, the membrane was then incubated 2 h at 25C with goat anti-rabbit IgG/HRP conjugate (Santa Cruz) in blocking buffer (1:100,000). Finally, after washing again in TBST, the membrane was placed in a plastic pouch for incubation with chemiluminescent reagent (Pierce Super-Signal WestFemto Maximum Sensitivity Substrate) for 5 min for subsequent analysis on a Kodak digital science" image station 440 CF. After densitometry, the nitrocellulose membrane was kept in the plastic pouch and in the dark at 25 °C overnight, before reprobing for β-actin as a control for sample loading onto the gels. The membrane was washed with TBST, and incubated 2 h at 25 °C with mouse monoclonal anti-β-actin antibody (Sigma) in blocking buffer (1:50,000). After incubation for 1 h at 25 °C with HRPconjugated goat polyclonal anti-mouse

IgG (Santa Cruz) in blocking buffer (1:100,000), the membrane was washed in TBST and processed for analysis as before.

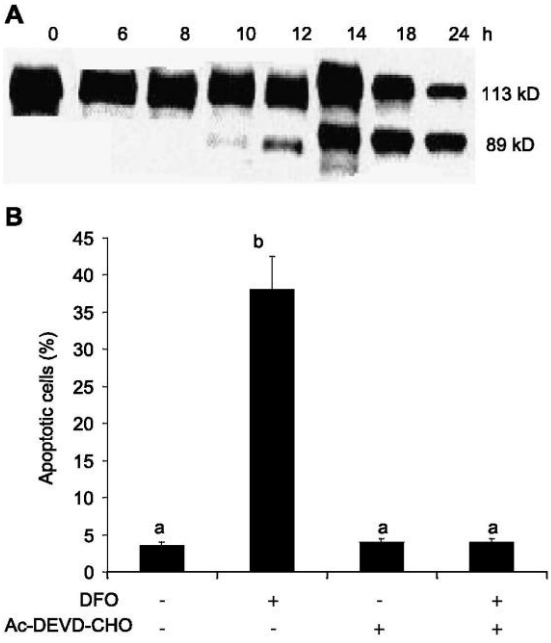

Fig. 2. Detection of proteolytic cleavage of PARP in DFO-treated Jurkat T-lymphocytes (A) and prevention of DFO-induced apoptosis by the selective caspase-3 inhibitor, Ac-DEVD-CHO (B). In (A), cells (2×10^6) were incubated with 100 μM DFO for different times as noted above. After SDS-PAGE/Western-blotting, PARP appeared as a single band with an apparent molecular mass of 113 kDa. The main cleavage product of PARP was detected as a secondary band of 89 kDa. The results are representative of three different experiments. In (B), cells (5×10^5) were pre-incubated without (−) or with (+) 600 μM Ac-DEVD-CHO for 3 h. These cells were then incubated without (−) or with (+) 100 μM DFO for 14 h. They were scored for the presence of morphological features characteristic of apoptosis (% apoptotic cells). Values are the means ± S.E., $n=3$. $^{b}P<0.01$ compared to other treatments.

2.7. Assessment of DNA damage

Single-strand breaks in DNA were assessed in the cells by the comet assay, as previously described [13]. Basically, cells resuspended in agarose gel were cast onto glass slides. Following treatment of the supported cells with alkaline detergent to remove membranes, the resulting nucleoids were subjected to electrophoresis. Nucleoid DNA was stained with ethidium bromide to permit visualization by fluorescence microscopy.

2.8. Statistical analysis of data

Where applicable, data were analyzed for statistical differences by analysis of variance (ANOVA) using a standard SAS program (version 6.12).

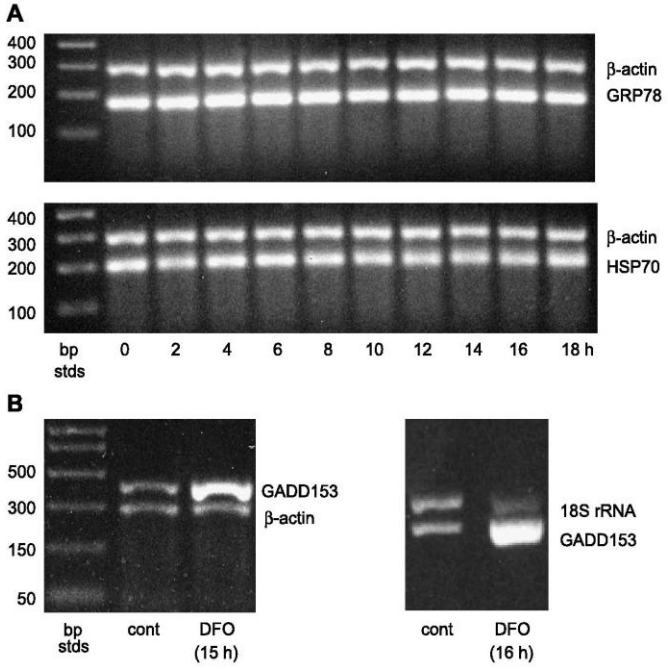

Fig. 3. Expression of GRP78, HSP70, and GADD153 mRNA in Jurkat T-lymphocytes after induction of iron deficiency with DFO. In (A), Jurkat T-lymphocytes were incubated with 100 μM deferoxamine (DFO) for multiple time points up to 18 h. Total RNA was isolated from the harvested samples for multiplex relative RT-PCR analysis of mRNA using gene specific primers for the target genes, GRP78 and HSP70, and internal control gene, β-actin. In (B), cells were exposed to 100 μM DFO for either 15 (left gel) or 16 h (right gel). Total RNA was isolated for the determination of GADD153 and the two internal control genes, β-Actin and 18S rRNA.

3. Results

3. 1. Morphological changes in iron-deficient cells

Upon examination by phase-contrast light microscopy (Fig. 1A), control or iron-sufficient cells were whole with smooth surface membranes. From this single view alone, none of the cells had irregular morphology. Nevertheless, after total scoring, about 5% of control cells were judged to have a morphological appearance characteristic of apoptosis, which is a percentage typically expected in culturing Jurkat T-lymphocytes. In contrast, many of the DFO-treated cells looked irregular. That is, after total scoring, about 40% of the cells were shrunken, had blebbing surface membranes, and/ or were in the process of breaking up into small apoptotic bodies. After DAPI-staining of the cells for examination by fluorescence microscopy (Fig. 1B), it can be seen that chromatin was mainly intact in nuclei of control cells, in marked contrast to the chromatin in many of the DFO-treated cells. More specifically, after total scoring, 2% of control cells and 48% of DFO-treated cells had chromatin condensation and/or fragmentation. Thus, these particular findings provide further morphological evidence of apoptosis in iron-deficient Jurkat T-lymphocytes.

3.2. Degradation of PARP in iron-deficient cells

In popular models of apoptosis [7], caspases are activated to function in the enzymatic degradation of numerous intracellular proteins having vital metabolic roles. PARP, which is involved in DNA repair, is a primary example of a protein degraded or cleaved by activated caspases during apoptosis [14]. Accordingly, to determine if PARP cleavage occurred in DFO-treated Jurkat T-lymphocytes, Western-blotting analysis was performed (Fig. 2A). PARP was detected as a band with an apparent molecular mass of 113 kDa. Following exposure of cells to DFO, a PARP cleavage product having an apparent molecular mass of 89 kDa was also detected. This product was not detectable until 10 h after exposing the cells to DFO, with peak appearance between 14 and 18 h. Therefore, the occurrence of PARP cleavage in the iron-deficient Jurkat T-lymphocytes strongly suggested that caspases could have been activated because caspases are known to be responsible for PARP cleavage [15,16].

3.3. Requirement for caspase-3 in mediating cell death induced by DFO

Morphological features of apoptosis are known to become apparent as a result of caspase-3 action [8]. Furthermore, caspase-3 is known to recognize PARP as a substrate and catalyze its cleavage [14]. Hence, to determine the requirement for caspase-3 in mediating cell death in iron-deficient Jurkat T-lymphocytes, we utilized the selective caspase-3 inhibitor, Ac-DEVD-CHO [17]. As shown in Fig. 2B, less than 5% of the control cells (i.e., cells not treated with DFO and/or Ac-DEVD-CHO) showed morphological evidence of apoptosis. However, more than 35% of the cells exposed to DFO had apoptotic morphology, but pretreating cells with Ac-DEVD-CHO prevented this effect by DFO. The eventual longer-term fate of these caspase-3 inhibitor-treated, iron-deficient cells was not determined. However, it is likely that they would not survive without a source of iron. Thus, it is conceivable that either necrosis occurs or a caspase-3-independent cell death pathway is initiated in such cells.

3.4. Effect of cellular iron deficiency on GRP78, HSP70, and GADD153 mRNA expression

GRP78 and HSP70 are two stress genes that are frequently activated in cells as an early response to being exposed to a stressful environment. Because making cells iron-deficient likely stresses them, GRP78 and HSP70 mRNA expression was determined in iron-deficient Jurkat T-lymphocytes (Fig. 3A). As can be seen, cellular iron deficiency induced by DFO did not change mRNA expression of either GRP78 (top gel) or HSP70 (bottom gel) when evaluated for periods up to 18 h after initially treating the cells with DFO. In contrast, there was increased expression of GADD153 mRNA, which was detectable by 10 h (data not shown) but with peak expression occurring at 15–16 h as shown by the representative results from two different experiments (Fig. 3B).

To provide further support that the effect of DFO on GADD153 mRNA expression was due to iron deprivation, two other compounds generally recognized as iron chelators were tested. Either 2,2-dipyridyl (DPD) or diethylenetriaminepentaacetic acid (DTPA) increased GADD153 mRNA expression as well in Jurkat T-lymphocytes (Fig. 4A). To determine whether the changes in GADD153 mRNA levels reflected changes in

GADD153 protein levels, Western immunoblotting analysis was performed. As can be seen (Fig. 4B), DFO, DPD, and DTPA each induced GADD153 protein expression. In the case of DFO, it was further found that co-treating Jurkat T-lymphocytes with 100 μM DFO and 50 μM ferrous sulfate prevented up-regulation of GADD153 mRNA and protein expression (Fig. 4A and B), suggesting that the effect of DFO on GADD153 mRNA expression was due to chelation of iron and not other metal ions.

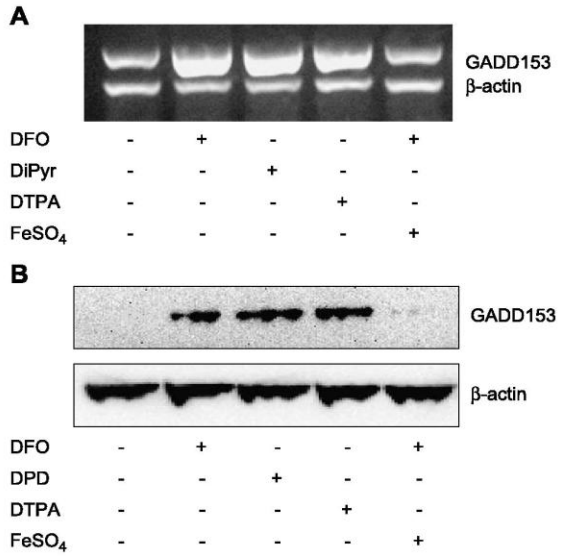

Fig. 4. Expression of GADD153 mRNA and protein in Jurkat T-lymphocytes after induction of iron deficiency. Cells were incubated with 100 μM DFO, DPD, or DTPA for 16 h. Other cells were co-incubated with 100 μM DFO and 50 μM ferrous sulfate for 16 h. Then, GADD153 and β-actin mRNA expression levels were determined by multiplex relative RT-PCR analysis (A). GADD153 and β-actin protein expression levels were determined by Western-immunoblotting analysis (B).

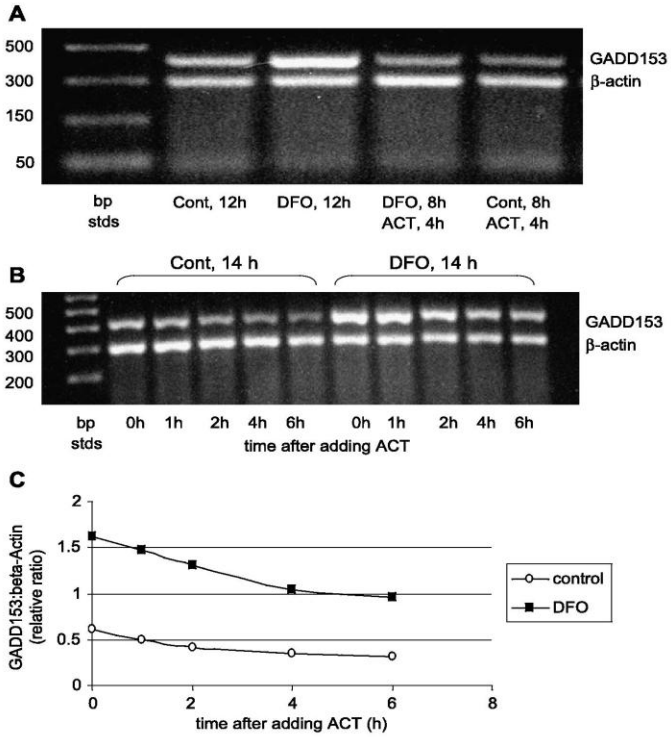

Fig. 5. Influence of DFO on GADD153 mRNA expression at the transcriptional and posttranscriptional levels as evaluated with actinomycin D. In (A), cells were incubated with 100 μM DFO for 8 h. Then, 5 μg/ml actinomycin D (ACT) was added and the incubation continued for another 4 h before subsequent multiplex relative RT-PCR analysis for GADD153 and β-actin mRNA expression levels. In (B), cells were incubated with 100 μM DFO for 14 h. Then, 1 μg/ml actinomycin D (ACT) was added to the cultures, and the incubation continued for periods up to 6 h before subsequent multiplex relative RT-PCR analysis for GADD153 and β-actin mRNA expression levels. In (C), the data from B were analyzed by densitometry to generate the figure shown that compares GADD153 mRNA rate of degradation in control and DFO-treated cells.

3.5. Evidence that the increased GADD153 mRNA expression caused by DFO is at the level of transcription

To come up with a fundamental explanation for the increased GADD153 mRNA expression in iron-deficient Jurkat T-lymphocytes, a standard experiment utilizing actinomycin D (ACT) was performed to inhibit or block transcription (Fig. 5A). Cells in complete culture media were incubated first with DFO for 8 h. Then, ACT was added, and the incubation continued for 4 h. As can be seen by the data, exposing cells to only DFO increased

GADD153 mRNA expression (lane 3) when compared to control cells (lane 2). This effect by DFO was prevented when cells were treated with ACT after being exposed to DFO (lane 4). In other experiments, GADD153 mRNA stability was not different between control cells and cells exposed to DFO, as can be seen in comparing GADD153 mRNA expression levels over the course of 6 h after blocking transcription with ACT following the exposure of cells to DFO for 14 h (Fig. 5B). Moreover, after densitometric analysis of the Fig. 5B data and subsequent plotting, no notable difference in the rate of GADD153 mRNA decay can be seen when comparing the relative slopes of the plots for control versus DFO-treated cells (Fig. 5C).

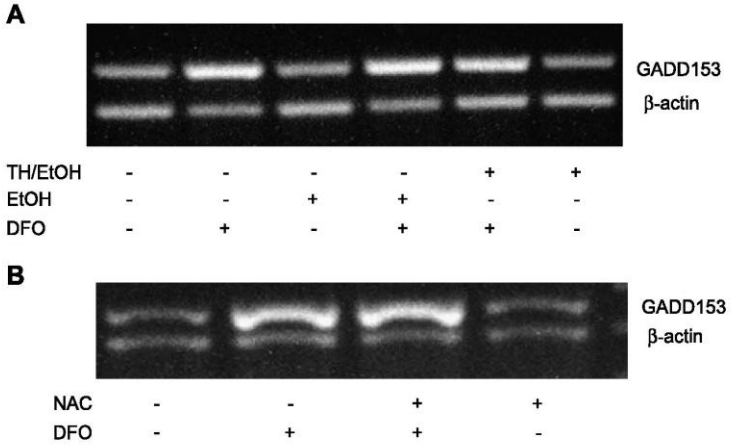

Fig. 6. Effect of antioxidants on DFO-induced up-regulation of GADD153 mRNA expression. In (A), cells were pretreated with either 100 μM α-tocopherol dissolved in absolute ethanol (TH/EtOH) or the solvent alone (EtOH) for 24 h. In (B), cells were pretreated with 20 mM *N*-acetylcysteine (NAC) for 2 h. After the cells were exposed to DFO for 15–16 h, multiplex relative RT-PCR analysis for GADD153 and β-actin mRNA was performed.

3.6. Evaluation of oxidative stress in contributing to up-regulation of GADD153 mRNA expression

Because GADD153 is often activated as a result of oxidative stress and DNA damage, the effect of antioxidants on GADD153 mRNA levels was determined. Pretreatment of Jurkat T-lymphocytes with either α-tocopherol (Fig. 6A) or N-acetylcysteine (Fig. 6B) failed to prevent DFO-induced up-regulation of GADD153 mRNA expression, suggesting that reactive oxygen species were not involved in GADD153 mRNA up-regulation. Furthermore, as assessed by the comet assay, single-strand breaks in DNA were not detected in DFO-treated Jurkat T-lymphocytes (Fig. 7), suggesting that oxidative DNA damage was not promoted by cellular iron deficiency, and hence, could not have led to up-regulation of GADD153 mRNA expression. As the rest of the data show, DFO actually inhibited H_2O_2-induced DNA damage to a large extent, likely because DFO chelated intracellular iron, which otherwise can react with H_2O_2 to form hydroxyl radical that ultimately damages cellular DNA.

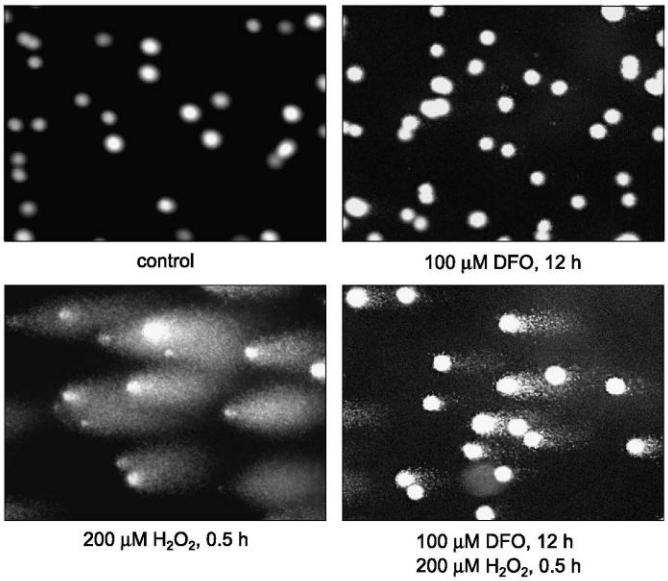

Fig. 7. Assessment of DNA damage in DFO-treated Jurkat-T lymphocytes. Cells were exposed to DFO (upper right) or to H_2O_2 as a positive control (lower left). The effect of DFO in potentially inhibiting H_2O_2-induced DNA damage was also examined (lower right). In this case, cells were pre-exposed to DFO before exposing to H_2O_2. Single-strand breaks in DNA were assessed by the comet assay.

4. Discussion

In the current study, DFO was the primary iron chelator utilized to make Jurkat T-lymphocytes iron-deficient. Cellular uptake of DFO occurs by endocytosis [18]. Subsequently, the DFO compartmentalizes largely in lysosomes, which contain a sizable pool of redox-active iron originating apparently from lysosomal proteolysis of iron-containing proteins [19]. Hence, this free iron in lysosomes, which may help meet the overall needs of the cell, is chelated by DFO. The unavailability or deficiency of iron induced by DFO can result in cell death. For example, HL-60 cells died when these cells were made iron-deficient by exposing them to DFO [5]. Such cell death was suggested to have occurred by way of apoptosis, based on the observation of a few cellular features characteristic of apoptosis. In support of this previous study [5], the present study found that DFO, or the iron deficiency caused by DFO, caused morphological features characteristic of apoptosis to appear in Jurkat T-lymphocytes. At least 10–12 h of exposure of the cells to DFO was required before any cell shrinkage, membrane blebbing, apoptotic bodies, and chromatin condensation and fragmentation were detectable. To expand these basic observations, the present results suggest that DFO-induced iron deficiency caused cell death in Jurkat T-lymphocytes via a caspase-3 -dependent pathway leading to apoptosis. Two lines of evidence support this view. First, cleavage of PARP was detected in DFO-treated cells. It is well established that PARP can be cleaved by caspase-3 [14]. Second, the morphological changes caused by DFO were not seen in Jurkat T-lymphocytes that were pretreated with the caspase3 inhibitor, Ac-DEVD-CHO, prior to their subsequent exposure to DFO. This finding is consistent with the results of other investigators [8] who reported that caspase-3 activity is required for the morphological changes associated with apoptosis.

The upstream events leading to activation of caspase-3 in DFO-treated Jurkat T-lymphocytes remain unknown. However, based on two popular models for apoptosis [7], the DFO-induced cell death could have been initiated via either of two apoptotic pathways. Basically, in the cell surface death receptor pathway, trimerization of cell surface receptors, such as FAS (CD95), leads to activation of initiator caspases, such as caspase-8. In turn, caspase-8 activates the effector caspase known as caspase-3, which is the main executioner of cells [20]. Activated caspase-3 ultimately commits the cell to death by cleaving p21 [21], thereby removing the p21 that promotes cell cycle arrest. On the other hand, in the mitochondria-mediated cell death pathway, disruption of mitochondrial membrane potential and structural integrity occurs initially. These events permit release of cytochrome *c*, which, along with Apaf-1 and (d)ATP, forms the apoptosome. This complex activates caspase-9, which in turn activates caspase-3. Thus, no matter which cell death pathway is followed by iron-deficient Jurkat T-lymphocytes, caspase-3 would be pivotal for the process of apoptosis since the cell surface death receptor pathway and mitochondria-mediated cell death pathway converge to result in the activation of caspase-3.

By exposing Jurkat T-lymphocytes to DFO, it is likely that this treatment created a stressful cellular environment because the cells were deprived of a critical micronutrient needed for their vitality and viability. As such, it would be expected that stress-response genes become activated in helping the iron-deficient cells to either survive or terminate. Although GRP78 and HSP70 mRNA expression was not affected by the cellular iron deficiency induced by DFO, an important member of the GADD was up-regulated. More specifically, GADD153 mRNA expression was increased, which could be potentially due to increased transcription or greater mRNA stability. Depriving cells of leucine [22] increased GADD153 mRNA expression, which was attributed to increased transcription and mRNA stability. Glutamine deprivation also induced GADD153 mRNA expression [23], but the primary mechanism was through mRNA stabilization. The increased GADD153 mRNA in iron-deficient Jurkat T-lymphocytes seemed to be at the level of transcription based on two observations. First, actinomycin D prevented the increased GADD153 mRNA expression caused by DFO. Second, GADD153 mRNA stability was not different in untreated versus DFO-treated Jurkat T-lymphocytes.

GADD genes are typically activated when cells are subjected to various forms of stress. For example, GADD mRNA expression increased in cells upon exposure to stress-inducing agents, such as peroxynitrite [24], UV radiation [25], and anti-cancer drugs [26], which also are known to induce DNA damage. Most interesting and relevant to the current effects of cellular iron deficiency on GADD153 mRNA expression, depriving cells of individual nutrients such as leucine [22], glutamine [23], glucose [27], and zinc [28] created a cellular environment that led to increased GADD153 gene expression. The molecular cascade leading to GADD153

gene activation is known to involve mitogen-activated protein kinases (MAPK). When p38/SAPK2 was activated by anisomycin in Jurkat T-lymphocytes, the levels of GADD153 transcript increased, but this effect was nullified with a selective chemical inhibitor of p38/SAPK2 [29].

Although cellular DNA damage can result in up-regulation of GADD153 gene expression, it is important to note that up-regulation of GADD gene expression does not necessarily occur merely as a consequence of growth arrest or DNA damage. Indeed, regarding the latter situation, single-strand breaks in DNA as assessed by the comet assay were not detected in DFO-treated Jurkat T-lymphocytes. This finding suggests that DFO did not induce oxidative stress, at least to a sufficient extent to cause single-strand breaks in DNA. Instead, it was found that DFO had the capability to inhibit H_2O_2-induced DNA damage in Jurkat T-lymphocytes. In inducing DNA damage, it is generally believed that H_2O_2 diffuses through cellular membranes, including the nuclear membrane. The incoming H_2O_2 reacts with transition metals such as ferrous ions that are in close proximity or loosely bound to DNA, resulting in the formation of hydroxyl radicals that cause oxidative damage to DNA. However, a series of recent studies [19,30,31] have advanced the concept that H_2O_2 enters lysosomes and reacts with redox-active iron originating from lysosomal degradation of metalloproteins. The hydroxyl radicals formed then cause rupture of the lysosomes. This allows some of the redox-active iron to reach the nucleus and react with H_2O_2 to form hydroxyl radicals that damage DNA. Consequently, cell cycle arrest and/or apoptosis occur. All of these events induced by H_2O_2 can be prevented by DFO, which has been attributed to the capacity of DFO to chelate redox-active iron in the lysosomal but also endosomal compartments of the cell [19,30,31].

The function of the GADD153 gene product is not completely known. However, GADD153 protein belongs to the CCAAT/enhancer binding protein (C/EBP) family of transcription factors [32]. There is evidence that GADD153 is directly involved in triggering apoptosis, based primarily on the finding that targeted overexpression of a GADD153 vector in several different cell lines resulted in apoptosis [33]. Furthermore, several recent studies [26,34–36] have suggested that the increased GADD153 gene expression caused by various inducers of apoptosis somehow triggers the critical early events leading to the initiation of apoptosis. Therefore, because there is substantial evidence to support the concept that GADD153 has a role in triggering apoptosis, it is conceivable that the increased GADD153 protein expression in iron-deficient Jurkat T-lymphocytes could be involved in triggering apoptosis in these cells. This is not to say, however, that other apoptosis-related genes or gene products are unimportant in the apoptosis induced by DFO. In particular, one study has suggested a potential role for the Bcl-2 gene family, based on the finding that DFO induced apoptosis in MCF-7 human breast cancer cells, in association with changes in the expression of the pro-apoptotic Bax gene and the anti-apoptotic Bcl-2 gene [9]. Thus, besides GADD153 gene expression being changed, it is possible that Bax and Bcl-2 gene expression was changed as well in DFO-treated Jurkat T-lymphocytes in helping to trigger apoptosis.

In conclusion, DFO-induced iron deficiency in Jurkat T-lymphocytes caused caspase-3-dependent programmed cell death, in association with increased GADD153 mRNA expression that was due to increased transcription rather than increased stability. The effect of cellular iron deficiency on GADD153 mRNA did not seem to involve reactive oxygen species, and, accordingly, was not a consequence of oxidative DNA damage. Because GADD153 protein was expressed as a result of treating the cells with DFO, a possible role for GADD153 in triggering DFO-induced apoptosis is under investigation.

References

[1] A.V. Hoffbrand, K. Ganeshaguru, J.W.L. Hooton, M.N.H. Tattersall, Effect of iron deficiency and deferroxamine on DNA synthesis in human cells, Br. J. Haematol. 33 (1976) 517–526.
[2] A. Jordan, P. Reichard, Ribonucleotide reductases, Ann. Rev. Biochem. 67 (1998) 71–98.
[3] S. Tomoyasu, K. Fukuchi, K. Yajima, K. Watanabe, H. Suzuki, K. Kawakami, K. Gomi, N. Tsuruoka, Suppression of HL-60 cell proliferation by deferoxamine: changes in c-myc expression, Anticancer Res. 13 (1993) 407–410.
[4] K. Fukuchi, S. Tomoyasu, H. Watanabe, S. Kaetsu, N. Tsuruoka, K. Gomi, Iron deprivation results in an increase in p53 expression, Biol. Chem. Hoppe-Seyler 376 (1995) 627–630.

[5] K. Fukuchi, S. Tomoyasu, N. Tsuruoka, K. Gomi, Iron deprivation-induced apoptosis in HL-60 cells, FEBS Lett. 350 (1994) 139–142.
[6] R.U. Haq, J.P. Wereley, C.R. Chitambar, Induction of apoptosis by iron deprivation in human leukemic CCRF-CEM cells, Exp. Hematol. 23 (1995) 428–432.
[7] I. Budihardjo, H. Oliver, M. Lutter, X. Luo, X. Wang, Biochemical pathways of caspase activation during apoptosis, Annu. Rev. Cell Dev. Biol. 15 (1999) 269–290.
[8] R.U. Janicke, M.L. Sprengart, M.R. Wati, A.G. Porter, Caspase-3 is required for DNA fragmentation and morphological changes associated with apoptosis, J. Biol. Chem. 273 (1998) 9357–9360.
[9] X.P. Jiang, F. Wang, D.C. Yang, R.L. Elliott, J.F. Head, Induction of apoptosis by iron depletion in the human breast cancer MCF-7 cell line and the 13762NF rat mammary adenocarcinoma in vivo, Anticancer Res. 22 (2002) 2685–2692.
[10] J. Kovar, P. Seligman, E.W. Gelfand, Lymphocyte lines under iron-depriving conditions: transferrin receptor expression related to various growth responses, Immunol. Lett. 42 (1994) 123–127.
[11] A. Samali, A.M. Gorman, T.G. Cotter, Apoptosis: the story so far, Experientia 52 (1996) 933–941.
[12] H.C. Mertani, T. Zhu, E.L. Goh, K.O. Lee, G. Morel, P.E. Lobie, Autocrine human growth hormone (hGH) regulation of human mammary carcinoma cell gene expression. Identification of CHOP as a mediator of hGH-stimulated human mammary carcinoma cell survival, J. Biol. Chem. 276 (2001) 21464–21475.
[13] A. Powolny, G. Loo, Deoxycholate induces DNA damage and apoptosis in human colon epithelial cells expressing either mutant or wild-type p53, Int. J. Biochem. Cell Biol. 33 (2001) 193–203.
[14] P.J. Duriez, G.M. Shah, Cleavage of poly(ADP-ribose) polymerase: a sensitive parameter to study cell death, Biochem. Cell. Biol. 75 (1997) 337–349.
[15] D.W. Nicholson, A. Ali, N.A. Thornberry, J.P. Vaillancourt, C.K. Ding,
M. Gallant, Y. Gareau, P.R. Griffin, M. Labelle, Y.A. Lazebnik, Identification and inhibition of the ICE/CED-3 protease necessary for mammalian apoptosis, Nature 376 (1995) 37–43.
[16] Z. Dong, P. Saikumar, J.M. Weinberg, M.A. Venkatachalam, Internucleosomal DNA cleavage triggered by plasma membrane damage during necrotic cell death. Involvement of serine but not cysteine proteases, Am. J. Pathol. 151 (1997) 1205–1213.
[17] V. Gurtu, S.R. Kain, G. Zhang, Fluorometric and colorimetric detection of caspase activity associated with apoptosis, Anal. Biochem. 251 (1997) 98–102.
[18] H. Cable, J.B. Lloyd, Cellular uptake and release of two contrasting iron chelators, J. Pharm. Pharmacol. 51 (1999) 131–134.
[19] Z. Yu, H.L. Persson, J.W. Eaton, U.T. Brunk, Intralysosomal iron: a major determinant of oxidant-induced cell death, Free Radic. Biol. Med. 34 (2003) 1243–1252.
[20] M.R. Wilson, Apoptosis: unmasking the executioner, Cell Death Differ. 5 (1998) 646–652.
[21] Y. Zhang, N. Fugita, T. Tsuruo, Caspase-mediated cleavage of p21 converts cancer cells from growth arrest to undergoing apoptosis, Oncogene 18 (1999) 1131–1138.
[22] A. Bruhat, C. Jousse, X.-Z. Wang, D. Ron, M. Ferrara, P. Fafournoux, Amino acid limitation induces expression of CHOP, a CCAAT/enhancer binding protein-related gene, at both transcriptional and post-transcriptional levels, J. Biol. Chem. 272 (1997) 17588–17593.
[23] S.F. Abcouwer, S. Schwarz, R.A. Meguid, Glutamine deprivation induces the expression of GADD45 and GADD153 primarily by mRNA stabilization, J. Biol. Chem. 274 (1999) 28645–28651.
[24] K. Oh-Hashi, W. Maruyama, K. Isobe, Peroxynitrite induces GADD34, 45, and 153 via p38 MAPK in human neuroblastoma SH-SY5Y cells, Free Radic. Biol. Med. 30 (2001) 213–221.
[25] T. Tong, W. Fan, H. Zhao, S. Jin, F. Fan, P. Blanck, I. Alomo, B. Rajasekaran, Y. Liu, N.J. Holbrook, Q. Zhan, Involvement of the
MAP kinase pathways in induction of GADD45 following UV radiation, Exp. Cell Res. 269 (2001) 64–72.
[26] D.-G. Kim, K.-R. You, M.-J. Liu, Y.-K. Choi, Y.-S. Won, GADD153- mediated anticancer effects of N-(4-hydroxyphenyl)retinamide on human hepatoma cells, J. Biol. Chem. 277 (2002) 38930–38938.
[27] S.G. Carlson, T.W. Fawcett, J.D. Bartlett, M. Bernier, N.J. Holbrook, Regulation of the C/EBP-related gene gadd153 by glucose deprivation, Mol. Cell. Biol. 13 (1993) 4736–4744.

[28] J.C. Fanzo, S.K. Reaves, L. Cui, L. Zhu, J.Y.J. Wu, Y.R. Wang, K.Y. Lei, Zinc status affects p53, gadd45, and c-fos expression and caspase-3 activity in human bronchial epithelial cells, Am. J. Physiol., Cell Physiol. 281 (2001) C751–C757.
[29] M. Rolli-Derkinderen, M. Gaestel, P38/SAPK2-dependent gene expression in Jurkat T cells, Biol. Chem. 381 (2000) 193–198.
[30] H.L. Persson, Z. Yu, O. Tirosh, J.W. Eaton, U.T. Brunk, Prevention of oxidant-induced cell death by lysosomotropic iron chelators, Free Radic. Biol. Med. 34 (2003) 1295–1305.
[31] P.T. Doulias, S. Christoforidis, U.T. Brunk, D. Galaris, Endosomal and lysosomal effects of desferrioxamine: protection of HeLa cells from hydrogen peroxide-induced DNA damage and induction of cell-cycle arrest, Free Radic. Biol. Med. 35 (2003) 719–728.
[32] D. Ron, J.F. Habener, CHOP, a novel developmentally regulated nuclear protein that dimerizes with transcription factors C/EBP and LAP and functions as a dominant-negative inhibitor of gene transcription, Genes Dev. 6 (1992) 439–453.
[33] E.V. Maytin, M. Ubeda, J.C. Lin, J.F. Habener, Stress-inducible transcription factor CHOP/gadd153 induces apoptosis in mammalian cells via p38 kinase-dependent and–independent mechanisms, Exp. Cell Res. 267 (2001) 193–204.
[34] I. Lengwehasatit, A.J. Dickson, Analysis of the role of GADD153 in the control of apopotosis in NSO myloma cells, Biotechnol. Bioeng. 80 (2002) 719–730.
[35] K.J. Conn, W.W. Gao, M.D. Ullman, C. McKeon-O'Malley, P.B. Eisenhauer, R.E. Fine, J.M. Wells, Specific up-regulation of GADD153/CHOP in 1-methyl-4-phenyl-pyridinium-treated SHSY5Y cells, J. Neurosci. Res. 68 (2002) 755–760.
[36] Y. Xia, N.S. Wong, W.F. Fong, H. Tideman, Upregulation of GADD153 expression in the apoptotic signaling of N-(4-hydroxyphenyl)retinamide (4HPR), Int. J. Cancer 102 (2002) 7–14.